HAWAII INSTITUTE FOR ASTRONOMY REPRINT 1182

THE ASTRONOMICAL JOURNAL VOLUME 96, NUMBER 6 DECEMBER 1988

CIRCUMSTANCES FOR PLUTO–CHARON MUTUAL EVENTS IN 1989

David J. Tholen and Marc W. Buie[a)]

Institute for Astronomy, University of Hawaii, 2680 Woodlawn Drive, Honolulu, Hawaii 96822

Received 26 August 1988

ABSTRACT

Circumstances are tabulated for 90 Pluto–Charon mutual events occurring during the 1989 opposition. The deepest and longest events will occur near postopposition quadrature in early August, when superior events will barely miss being total. Our most recent determination of the orbital and physical parameters for the Pluto–Charon system has not changed substantially from last year's determination, although the uncertainties in the parameters have decreased by about a factor of 2. Two new stars have been selected as comparison stars for events occurring before opposition in 1989. The primary star is located at R. A. $15^h06^m52^s.15$ and Dec. $-00°43'26''.5$, and the check star is located at R. A. $15^h05^m51^s.65$ and Dec. $-00°55'16''.4$ (mean equator and equinox of 1950.0). The 1988 comparison stars should be utilized for events occurring after opposition. Standardization of the comparison star 1988 Primary has yielded the following preliminary magnitudes: $B = 12.2571 \pm 0.0006$ and $V = 11.3285 \pm 0.0010$.

I. INTRODUCTION

During 1988, we observed the tenth anniversary of the discovery of Pluto's satellite, Charon. That discovery alone was responsible for renewing substantial interest in the solar system's outermost planet, but more importantly, Pluto and Charon became an eclipsing binary system only a scant 6.5 yr after the discovery of Charon. Given that such geometry can occur only twice during each 248 yr orbit of the Sun, Charon's discovery came at an incredibly fortuitous time.

Extensive observations of the transits and occultations that occurred during the first four years of the event season have enabled us to produce reliable physical and orbital parameters for the system. This knowledge has subsequently been applied to theoretical studies of Pluto and Charon. The net result has been a tremendous increase in our knowledge of this remote planetary system, all without the benefit of a spacecraft encounter.

In the Introduction to our 1988 circumstances paper (Tholen *et al.* 1987c), we listed a number of papers written in 1987 about the Pluto–Charon system. The publication rate of papers remains high. Mutual-event observational data have been or are in the process of being published by Birch *et al.* (1988), Binzel (1988), Tholen and Hubbard (1988), and Blanco *et al.* (1988). The effect of diffraction (or lack of it) on these events has been examined by Mulholland and Gustafson (1987) and Tholen and Hubbard (1988). Models for the surface-albedo distribution on Pluto have been computed by Marcialis (1988) and Buie and Tholen (1988); both models suggest that Pluto has two high-albedo polar caps and a dark equatorial region with a nonuniform longitudinal albedo distribution. A surface-color distribution for Pluto has been proposed by Binzel (1988). In an earlier paper (Tholen *et al.* 1987a), we proposed that Charon had hemispheres of two different colors as a means of explaining why the depths of superior events were wavelength dependent, whereas the depths of inferior events were not. With the aid of additional data, Binzel has suggested another possibility (which we now consider more likely), namely that Charon has a uniform neutral color over its surface, virtually the same as the color of Pluto's polar caps; the overall reddish color of Pluto is produced by its darker equatorial region. Such a surface-color distribution would account for the observed wavelength dependence seen in the depths of both inferior and superior events. Interior-structure models have been computed by McKinnon and Mueller (1988) and Simonelli *et al.* (1988); the estimated rock fraction for the bulk composition of Pluto has been placed in the 60% to 80% range.

On 1988 June 9 UT, Pluto occulted a star. Numerous observations were obtained of the rare event by astronomers in Australia, New Zealand, and aboard the *Kuiper Airborne Observatory*. Initial reports by Blow *et al.* (1988), Kilmartin *et al.* (1988), and Watson *et al.* (1988) all indicate irrefutable evidence for an extended atmosphere around Pluto. Hubbard *et al.* (1988) have performed an analysis of the data obtained from one of the sites; they have shown the occultation light curve to be consistent with a methane atmosphere of surface pressure ~ 10 μbar. Additional analyses of the occultation data are sure to be forthcoming in the very near future.

Although no more total events will occur, the observations of Pluto–Charon mutual events in 1989 are nevertheless very important. In Sec. II, we present the circumstances for 90 observable mutual events that occur during the 1989 opposition. Our latest model for the orbital and physical parameters of the system is described in Sec. III, and the extension of our comparison-star network to 1989 is discussed in Sec. IV. The kinds of information that can be extracted from observations in 1989, as well as other general comments, are mentioned in Sec. V. This paper is the fourth in a series, being preceded by similar papers that described the events in 1986 (Tholen 1985b), 1987 (Tholen *et al.* 1987b), and 1988 (Tholen *et al.* 1987c). These earlier papers will hereafter be referred to as Paper I, Paper II, and Paper III, respectively.

II. MUTUAL EVENTS IN 1989

The circumstances for Pluto–Charon mutual events occurring in 1989 are given in Table I. No total events will occur in 1989, so the columns containing the times of second and third contact (as in Paper II and Paper III) do not appear in the table. Otherwise, the format of this table is identical to that used in those earlier papers. The columns contain the following information:

Col. 1—UT date corresponding to the time of maximum depth (column 4).

Col. 2—Universal Time of first contact (beginning of event).

a) Current address: Space Telescope Science Institute, 3700 San Martin Drive, Baltimore, MD 21218.

 0004-6256/88/061977-06$00.90

TABLE I. Circumstances for Pluto–Charon mutual events occurring during the 1989 opposition.

	Contacts		Max. Depth		R.A. (1950.0)	DEC.	r	Δ	α	B	Windows		East Long.	Event
UT Date	First	Last	UT	Mag	h m s	° ′ ″	AU	AU	°	Mag	30°N	30°S	Range	Type
1988 Dec 10	15:30	19:34	17:25	0.32	15 02 02.1	−01 03 01	29.659	30.430	1.17	14.87	—	—	—	Inf
13	20:09	*00:12*	22:14	0.15	15 02 27.3	−01 04 02	29.659	30.398	1.24	14.76	—	—	—	Sup
17	00:49	04:50	02:42	0.31	15 02 51.7	−01 04 53	29.659	30.364	1.31	14.87	0:13	—	6- 70	Inf
20	05:28	09:28	07:31	0.15	15 03 15.4	−01 05 37	29.659	30.327	1.38	14.76	0:27	—	294- 0	Sup
23	10:09	14:06	11:59	0.30	15 03 38.2	−01 06 13	29.659	30.289	1.44	14.87	0:40	—	221-290	Inf
26	14:48	18:44	16:47	0.15	15 04 00.3	−01 06 41	29.659	30.248	1.51	14.76	0:54	—	148-221	Sup
29	19:29	23:22	21:16	0.29	15 04 21.3	−01 07 01	29.659	30.206	1.56	14.87	1:08	—	76-151	Inf
1989 Jan 02	00:08	04:00	02:04	0.14	15 04 41.5	−01 07 13	29.659	30.162	1.62	14.76	1:21	—	3- 82	Sup
05	04:46	08:38	06:34	0.28	15 05 00.6	−01 07 16	29.659	30.116	1.67	14.87	1:33	—	291- 12	Inf
08	09:24	13:15	11:20	0.14	15 05 18.6	−01 07 12	29.658	30.069	1.71	14.76	1:46	—	219-303	Sup
11	14:03	17:54	15:51	0.27	15 05 35.5	−01 06 59	29.658	30.020	1.76	14.86	1:59	0:05	144-233	Inf
14	18:41	22:31	20:36	0.14	15 05 51.2	−01 06 39	29.658	29.971	1.79	14.75	2:11	0:22	72-164	Sup
18	*23:20*	03:09	01:09	0.26	15 06 05.7	−01 06 11	29.658	29.920	1.82	14.86	2:23	0:39	359- 94	Inf
21	03:58	07:47	05:52	0.14	15 06 19.0	−01 05 35	29.658	29.869	1.85	14.75	2:34	0:55	286- 24	Sup
24	08:36	12:25	10:26	0.26	15 06 31.1	−01 04 52	29.658	29.817	1.87	14.85	2:46	1:11	213-314	Inf
27	13:14	17:02	15:08	0.13	15 06 41.8	−01 04 02	29.658	29.764	1.89	14.74	2:57	1:27	141-245	Sup
30	17:53	21:41	19:44	0.25	15 06 51.3	−01 03 04	29.658	29.711	1.90	14.85	3:08	1:44	68-175	Inf
Feb 03	*22:31*	02:18	00:24	0.13	15 06 59.4	−01 02 00	29.658	29.658	1.90	14.73	3:19	2:00	356-105	Sup
06	03:10	06:56	05:01	0.24	15 07 06.1	−01 00 50	29.658	29.604	1.90	14.84	3:29	2:16	283- 34	Inf
09	07:48	11:34	09:41	0.13	15 07 11.5	−00 59 33	29.658	29.551	1.90	14.72	3:39	2:32	211-324	Sup
12	12:26	16:12	14:18	0.24	15 07 15.5	−00 58 11	29.658	29.498	1.89	14.83	3:48	2:48	138-254	Inf
15	17:04	20:49	18:57	0.13	15 07 18.1	−00 56 43	29.658	29.446	1.87	14.72	3:58	3:04	66-184	Sup
18	21:43	*01:28*	23:35	0.23	15 07 19.4	−00 55 10	29.658	29.394	1.85	14.82	4:08	3:20	353-113	Inf
22	02:21	06:05	04:13	0.13	15 07 19.2	−00 53 32	29.657	29.343	1.82	14.71	4:18	3:35	281- 43	Sup
25	07:00	10:43	08:51	0.23	15 07 17.8	−00 51 50	29.657	29.293	1.79	14.81	4:27	3:51	208-332	Inf
28	11:38	15:21	13:29	0.12	15 07 15.0	−00 50 03	29.657	29.244	1.75	14.70	4:37	4:06	135-262	Sup
Mar 03	16:17	19:59	18:07	0.23	15 07 10.9	−00 48 14	29.657	29.196	1.71	14.80	4:46	4:21	63-191	Inf
06	20:55	*00:36*	22:45	0.12	15 07 05.5	−00 46 21	29.657	29.150	1.66	14.69	4:55	4:36	350-121	Sup
10	01:33	05:14	03:24	0.22	15 06 58.8	−00 44 25	29.657	29.105	1.61	14.79	5:04	4:52	278- 51	Inf
13	06:11	09:52	08:02	0.12	15 06 50.9	−00 42 28	29.657	29.062	1.55	14.68	5:13	5:07	205-340	Sup
16	10:50	14:30	12:40	0.22	15 06 41.8	−00 40 29	29.657	29.021	1.49	14.78	5:22	5:22	132-269	Inf
19	15:28	19:08	17:18	0.12	15 06 31.6	−00 38 28	29.657	28.981	1.43	14.66	5:30	5:37	60-199	Sup
22	20:07	23:46	21:56	0.21	15 06 20.3	−00 36 27	29.657	28.944	1.36	14.77	5:38	5:51	347-130	Inf
26	00:45	04:23	02:34	0.11	15 06 07.9	−00 34 26	29.657	28.909	1.29	14.65	5:47	6:06	275- 61	Sup
29	05:24	09:02	07:13	0.21	15 05 54.5	−00 32 25	29.657	28.876	1.22	14.76	5:55	6:21	202-351	Inf
Apr 01	10:02	13:39	11:51	0.11	15 05 40.2	−00 30 25	29.657	28.845	1.14	14.64	6:04	6:36	129-282	Sup
04	14:41	18:18	16:29	0.20	15 05 25.0	−00 28 26	29.657	28.817	1.07	14.75	6:12	6:50	56-213	Inf
07	19:20	22:55	21:07	0.11	15 05 09.0	−00 26 28	29.657	28.792	0.99	14.63	6:21	7:05	344-144	Sup
11	*23:59*	03:34	01:46	0.20	15 04 52.3	−00 24 33	29.657	28.769	0.91	14.74	6:29	7:20	271- 75	Inf
14	04:37	08:11	06:24	0.11	15 04 34.9	−00 22 41	29.657	28.749	0.84	14.63	6:38	7:35	198- 6	Sup
17	09:16	12:50	11:03	0.19	15 04 16.8	−00 20 52	29.657	28.732	0.77	14.73	6:47	7:49	125-296	Inf
20	13:54	17:27	15:41	0.10	15 03 58.3	−00 19 06	29.657	28.717	0.70	14.62	6:55	8:03	53-227	Sup
23	18:34	22:06	20:22	0.19	15 03 39.3	−00 17 25	29.656	28.705	0.64	14.72	7:04	8:17	340-157	Inf
27	*23:12*	02:44	00:58	0.10	15 03 19.9	−00 15 48	29.656	28.697	0.60	14.61	7:13	8:22	267- 86	Sup
30	03:51	07:26	05:41	0.19	15 03 00.2	−00 14 16	29.656	28.691	0.56	14.72	7:21	8:22	194- 13	Inf
May 03	08:29	12:07	10:15	0.10	15 02 40.3	−00 12 49	29.656	28.688	0.55	14.61	7:29	8:22	120-300	Sup
06	13:09	16:49	15:00	0.20	15 02 20.3	−00 11 28	29.656	28.687	0.55	14.72	7:25	8:21	47-227	Inf
09	17:47	21:30	19:37	0.10	15 02 00.2	−00 10 12	29.656	28.690	0.58	14.61	7:18	8:21	333-154	Sup
13	*22:27*	02:11	00:18	0.21	15 01 40.1	−00 09 03	29.656	28.696	0.62	14.72	7:11	8:21	260- 81	Inf
16	03:05	06:52	05:01	0.10	15 01 20.1	−00 08 01	29.656	28.704	0.67	14.62	7:04	8:20	186- 8	Sup
19	07:44	11:33	09:37	0.22	15 01 00.3	−00 07 06	29.656	28.716	0.73	14.73	6:54	8:19	113-295	Inf
22	12:23	16:14	14:25	0.11	15 00 40.8	−00 06 18	29.656	28.730	0.80	14.62	6:39	8:19	40-222	Sup
25	17:02	20:55	18:56	0.24	15 00 21.6	−00 05 37	29.656	28.747	0.88	14.74	6:24	8:18	327-149	Inf
28	21:41	*01:35*	23:44	0.12	15 00 02.7	−00 05 03	29.656	28.766	0.95	14.63	6:08	8:14	254- 76	Sup
Jun 01	02:21	06:16	04:14	0.26	14 59 44.4	−00 04 38	29.656	28.788	1.03	14.74	5:52	8:02	184- 3	Inf
04	06:59	10:56	09:03	0.13	14 59 26.6	−00 04 20	29.656	28.813	1.11	14.64	5:37	7:49	114-290	Sup
07	11:39	15:37	13:32	0.28	14 59 09.5	−00 04 10	29.656	28.840	1.18	14.76	5:22	7:36	44-217	Inf
10	16:18	20:17	18:21	0.14	14 58 53.0	−00 04 08	29.656	28.870	1.26	14.65	5:08	7:24	334-144	Sup
13	20:57	*00:57*	22:50	0.30	14 58 37.3	−00 04 15	29.656	28.902	1.33	14.77	4:53	7:11	264- 71	Inf
17	01:36	05:37	03:40	0.15	14 58 22.3	−00 04 30	29.656	28.936	1.40	14.66	4:38	6:58	194-358	Sup
20	06:16	10:17	08:08	0.31	14 58 08.3	−00 04 52	29.656	28.972	1.47	14.77	4:24	6:44	124-285	Inf
23	10:54	14:56	12:58	0.16	14 57 55.1	−00 05 23	29.656	29.010	1.53	14.67	4:11	6:31	54-212	Sup
26	15:34	19:37	17:26	0.33	14 57 43.0	−00 06 03	29.656	29.050	1.59	14.79	3:58	6:18	344-139	Inf
29	20:13	*00:16*	22:16	0.16	14 57 31.8	−00 06 50	29.656	29.092	1.65	14.68	3:45	6:04	275- 66	Sup
Jul 03	00:53	04:55	02:48	0.34	14 57 21.7	−00 07 45	29.656	29.135	1.70	14.80	3:33	5:50	205-353	Inf
06	05:31	09:34	07:34	0.17	14 57 12.6	−00 08 48	29.656	29.180	1.75	14.69	3:21	5:36	136-280	Sup
09	10:11	14:14	12:00	0.35	14 57 04.7	−00 09 59	29.656	29.226	1.79	14.81	3:09	5:22	66-207	Inf
12	14:50	18:53	16:52	0.17	14 56 58.0	−00 11 18	29.656	29.273	1.83	14.70	2:58	5:08	357-134	Sup
15	19:29	23:32	21:17	0.35	14 56 52.5	−00 12 43	29.656	29.321	1.86	14.82	2:47	4:54	287- 62	Inf
19	00:07	04:10	02:09	0.17	14 56 48.1	−00 14 17	29.656	29.370	1.89	14.71	2:36	4:40	218-349	Sup
22	04:46	08:49	06:35	0.36	14 56 45.1	−00 15 56	29.656	29.420	1.92	14.83	2:26	4:26	149-276	Inf
25	09:24	13:28	11:26	0.17	14 56 43.2	−00 17 44	29.655	29.471	1.94	14.72	2:17	4:12	79-203	Sup
28	14:03	18:07	15:52	0.36	14 56 42.7	−00 19 37	29.655	29.522	1.95	14.83	2:08	3:58	10-130	Inf
31	18:41	22:45	20:43	0.17	14 56 43.4	−00 21 36	29.655	29.574	1.96	14.73	1:59	3:44	301- 58	Sup
Aug 04	*23:20*	03:23	01:09	0.36	14 56 45.4	−00 23 42	29.655	29.625	1.96	14.84	1:49	3:30	232-345	Inf
07	03:58	08:01	06:00	0.17	14 56 48.7	−00 25 53	29.655	29.677	1.96	14.74	1:40	3:16	163-272	Sup
10	08:36	12:40	10:26	0.35	14 56 53.3	−00 28 10	29.655	29.729	1.95	14.85	1:32	3:02	93-200	Inf
13	13:14	17:17	15:16	0.17	14 56 59.2	−00 30 32	29.655	29.780	1.94	14.74	1:23	2:48	24-127	Sup
16	17:53	21:55	19:43	0.34	14 57 06.3	−00 32 58	29.655	29.831	1.92	14.86	1:15	2:34	315- 54	Inf
20	*22:31*	02:33	00:32	0.17	14 57 14.7	−00 35 28	29.655	29.881	1.90	14.75	1:06	2:20	246-342	Sup
23	03:10	07:11	05:01	0.33	14 57 24.3	−00 38 03	29.655	29.931	1.87	14.86	0:58	2:06	177-269	Inf
26	07:48	11:48	09:48	0.17	14 57 35.2	−00 40 41	29.655	29.980	1.84	14.75	0:50	1:53	108-196	Sup
29	12:26	16:26	14:18	0.32	14 57 47.3	−00 43 23	29.655	30.028	1.80	14.87	0:42	1:39	39-124	Inf
Sep 01	17:04	21:03	19:03	0.16	14 58 00.6	−00 46 08	29.655	30.075	1.76	14.76	0:34	1:25	330- 51	Sup
04	21:43	*01:40*	23:36	0.30	14 58 15.1	−00 48 55	29.655	30.121	1.71	14.87	0:26	1:11	261-338	Inf
08	02:21	06:17	04:19	0.15	14 58 30.7	−00 51 44	29.655	30.165	1.66	14.76	0:18	0:58	192-266	Sup
11	07:00	10:54	08:53	0.29	14 58 47.4	−00 54 35	29.655	30.208	1.61	14.87	0:11	0:45	124-193	Inf
14	11:38	15:31	13:34	0.15	14 59 05.2	−00 57 27	29.655	30.249	1.55	14.76	0:03	0:32	55-121	Sup
17	16:17	20:08	18:10	0.27	14 59 24.0	−01 00 20	29.655	30.288	1.49	14.87	—	0:19	346- 48	Inf
20	20:55	*00:44*	22:50	0.14	14 59 43.7	−01 03 14	29.655	30.326	1.43	14.76	—	0:06	277-336	Sup

Col. 3—Universal Time of last contact (end of event).

Col. 4—Universal Time of maximum event depth.

Col. 5—Approximate depth of event in Johnson *B*.

Col. 6—1950.0 right ascension of Pluto at the time given in column 4.

Col. 7—1950.0 declination of Pluto at the time given in column 4.

Col. 8—Heliocentric distance of Pluto in Astronomical Units.

Col. 9—Geocentric distance of Pluto in Astronomical Units.

Col. 10—Phase angle of Pluto in degrees.

Col. 11—Johnson *B* magnitude of the system (out of eclipse).

Col. 12—Window duration in hours and minutes for 30° north latitude.

Col. 13—Window duration in hours and minutes for 30° south latitude.

Col. 14—Range of east longitudes in degrees from which at least a portion of the event can be observed.

Col. 15—Type of event (Charon at inferior or superior conjunction).

In some instances, an event spans 0 hr UT; therefore some of the times listed in columns 2 and 3 do not refer to the date listed in column 1. If a time in column 2 is printed in italics, it refers to the time on the previous day; similarly, if a time in column 3 is printed in italics, it refers to the time on the following day.

The computations we used to determine the times of first and last contact were performed at a time resolution of 30 s, which is a factor of 2 higher than we used to compute the times of contacts for Paper II and Paper III. Nevertheless, the accuracy of the orbital and physical parameters is still the limiting factor in the accuracy of the times of contacts; the times should be good to better than 3 min for all events.

The depths of the superior events will be approximately correct if our assumptions about a uniform albedo over Charon are correct, and if the observations are made through a filter approximating Johnson *B*. Longer wavelengths will yield shallower depths, given the color difference for superior events found by Tholen *et al.* (1987a). On the other hand, the depths of the inferior events are somewhat uncertain, given Pluto's nonuniform surface-albedo distribution (Buie and Tholen 1988). For this particular set of circumstances, we used the albedo that reproduces the depth of the 1986 January 15 UT event. During that event, Charon transited the northern polar cap of Pluto, which we believe has a rather high albedo. (As in our earlier papers, we define north to lie in the direction of Pluto's angular-momentum vector.) During 1989, Charon and its shadow will be occulting the southern polar cap of Pluto. If the albedos of the northern and southern polar caps are roughly equal, then the depths listed in Table I should be approximately correct. Although the actual absolute depths of the events may differ somewhat from those tabulated, the relative depths (that is, the change in depth from one inferior event to the next) should be fairly accurate, unless there is a very sharp, high-contrast discontinuity in Pluto's surface-albedo distribution (which could indeed be the case).

The tabulated Johnson *B* magnitude is the brightness the system would have at the time of maximum depth if there were no event. If for some reason an observer is unable to obtain photometry of the system immediately prior to or following an event, then this value can be used to estimate the depth of the event. The Johnson *V* magnitude is 0.84 mag brighter than the *B* magnitude. The uncertainty in the magnitude is less than 0.02 mag.

As in Paper I, Paper II, and Paper III, we used 2.5 airmasses and astronomical twilight as the limits for defining the length of the observing window. Note that the 1988 December 10 and 13 events have no window as seen from either the northern or southern hemisphere. The December 10 event was included in the table because we can observe first contact from Mauna Kea at 3.1 airmasses, if observations are extended a few minutes into astronomical twilight. The December 13 event is included merely to maintain the continuity of the table.

We emphasize that the longitude range given in the penultimate column refers to east longitudes. Also, the inclusion of a particular longitude within the tabulated range means that at least a portion of the event can be observed from either 30° north or 30° south latitude, but not necessarily both.

The geometry of Pluto, Charon, and shadow is shown for both inferior and superior events in Fig. 1 for three representative times in 1989: preopposition quadrature, opposition, and postopposition quadrature. The effects of parallax are at their maximum near quadrature, with Charon's disk covering the southernmost latitudes on Pluto preopposition and the northernmost latitudes postopposition. Opposition represents the time when shadowing effects are at their minimum.

From one inferior event to the next, the position of Charon's shadow with respect to Pluto is slowly and monotonically moving from right to left (in Fig. 1) with increasing time; this motion is strictly due to Pluto's orbital motion around the Sun. On the other hand, between preopposition and postopposition quadrature (approximately), the position of Charon itself with respect to Pluto will be moving from left to right (or right to left from one superior event to the next); this motion is due to the Earth moving around its orbit (parallax). Before and after this interval, Charon moves more rapidly from right to left. With this information, one should be able to estimate the geometry for any particular event. For a look backward in time, see Fig. 1 of Paper III and Fig. 1 of Paper II.

III. THE MODEL FOR THE PLUTO–CHARON SYSTEM

The orbital and physical parameters used to generate these circumstances are shown in Table II. Data from 20 different events observed between 1985 February and 1988 May were used in the analysis. To avoid the possibility of having the model affected adversely by systematic differences between datasets, only the *B* filter data acquired at Mauna Kea were used to generate this model. Eventually, we expect to incorporate properly calibrated data obtained at other wavelengths from other sites. To compute the model parameters, a nonlinear least-squares fit was performed to 2007 data points; the mean residual between the observed brightness and the model prediction is only 0.008 mag.

To assess the uncertainties in the various model parameters, we divided the dataset into nine subsets of 223 observations each. A separate least-squares fit was performed on each subset; the result was nine sets of model parameters, from which we computed the mean and standard deviation of the mean for each parameter. Our experience has shown that the formal standard deviations derived via this technique tend to underestimate the true uncertainties in the

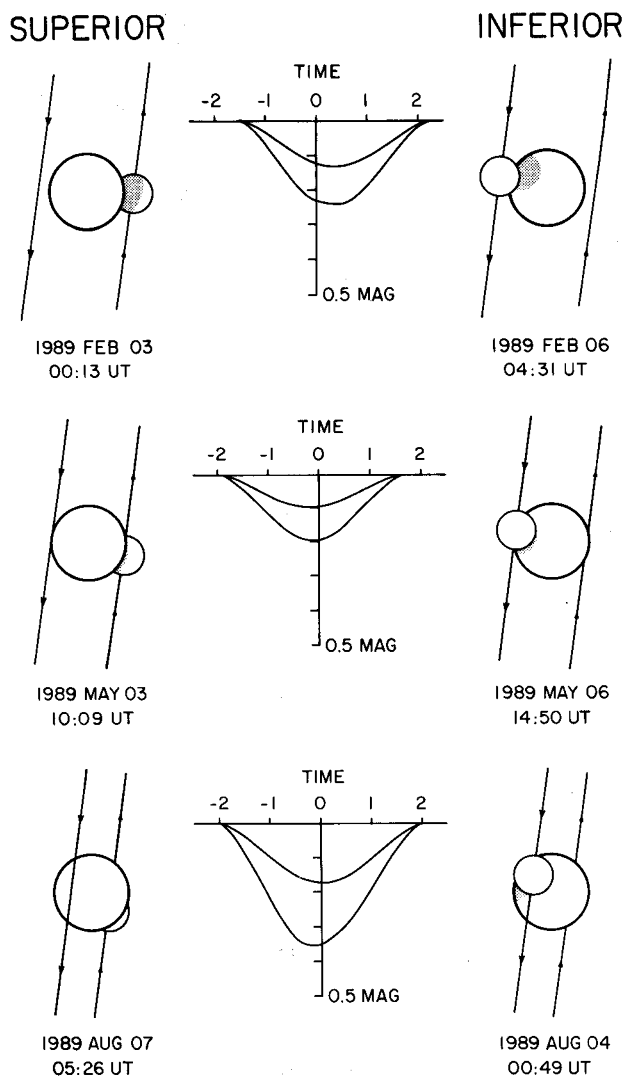

FIG. 1. The geometry of the Pluto–Charon system is shown in the leftmost and rightmost panels for three representative times in 1989: preopposition quadrature (top), opposition (middle), and postopposition quadrature (bottom). Equatorial north is up in all views. The middle vertical panel shows the predicted light-curve shapes for the inferior and superior event on either side. The time axis is in hours from geometric minimum separation between the projected disks of Pluto and Charon. The light curve is not symmetric about minimum separation because of the influence of the shadow cast by the body closer to the Sun. In all cases, the deeper of the two light curves corresponds to the inferior event depicted on the right, whereas the shallower light curve corresponds to the superior event depicted on the left.

model parameters because of, primarily, the assumptions used in the modeling process. For example, our modeling software currently assumes that there is no surface-albedo variegation on Charon; it also assumes that the phase functions for Pluto and Charon are identical. The effects of limb darkening have not yet been incorporated into the software; the albedo model of Buie and Tholen (1988) indicates that nonnegligible limb darkening may be present around the high-albedo portions of Pluto's projected circumference. These are all second-order effects, however; the gross shapes of the light curves are reasonably well matched (as evidenced by the small mean residual) by accounting for the geometrical blockage of the reflected light of one object by

TABLE II. Orbital and physical parameters used to generate the circumstances.

Semimajor axis	19,640 ± 320 km
Eccentricity	0.00009 ± 0.00038
Inclination[a]	98.3 ± 1.3 deg
Ascending node[a]	222.37 ± 0.07 deg
Argument of periapsis[a]	290 ± 180 deg
Mean anomaly[b]	259.90 ± 0.15 deg
Epoch	JDE 2,446,600.5 = 1986 June 19
Period	6.387230 ± 0.000021 days
Pluto radius	1142 ± 9 km
Charon radius	596 ± 17 km
Pluto blue geometric albedo	0.43–0.60
Charon blue geometric albedo	0.375 ± 0.018
Mean density	2.065 ± 0.047 g cm^{-3}

[a] Referred to the mean equator and equinox of 1950.0.
[b] Measured from the ascending node (see the text).

the other object and its shadow. The uncertainties associated with each model parameter in Table II reflect our best estimate of the realistic uncertainty in each parameter; they are *not* the formal standard deviations.

The range of geometric albedos for Pluto given in Table II reflects the variegation of Charon-sized regions of Pluto. At even smaller scales, we expect the albedo contrast to be even higher than indicated by this range.

The semimajor axis for Charon's orbit is based on speckle interferometric observations of the system (Beletic *et al.* 1988). This particular orbit solution for the semimajor axis was constrained to satisfy the mutual-event observations acquired through 1987. This new value for the semimajor axis is 2.7% larger than the one we had used previously (Tholen 1985a). Consequently, all linear dimensions for the system have been increased by the same amount, and the geometric albedos have been decreased to compensate. This scaling should be kept in mind when comparing our new model parameters with older ones. Our derived density, however, is independent of the value for the semimajor axis, given that both the mass, derived via Kepler's third law, and the volume go as the cube of linear dimensions.

We now have a sufficient amount of data to solve for the eccentricity of Charon's orbit. The time intervals between events make the solution sensitive to the alignment of the line of apsides perpendicular to the line of sight. Similarly, the relative durations of inferior and superior events make the solution sensitive to the alignment of the line of apsides parallel to the line of sight. Therefore, we can truly solve for the eccentricity itself, not just the eccentricity multiplied by the cosine of the periapsis angle. The computed value is still indistinguishable from zero, which justifies our earlier assumptions of a circular orbit for Charon. As expected, the argument of periapsis is completely indeterminate. Because of this, the mean anomaly in Table II has been measured from the ascending node, not from periapsis as is the usual practice.

The uncertainties in the radii of Pluto and Charon are relative to the assumed value for the semimajor axis and do not include the uncertainty in the semimajor axis. These values are given in Table II because they are the correct ones to use when propagating the error into the derived mean density of the system. If the uncertainty in the semimajor axis is included, both radii would have error bars of about 20 km.

IV. COMPARISON STARS

We have an ongoing program of selecting and standardizing comparison stars specifically for use by those observing

TABLE III. Comparison stars for use in 1989.

Star	R. A. (1950.0)	Dec.	B	$B-V$
1988 Primary	$14^h58^m05^s.92$	$+00°12'15''.2$	12.257	0.928
1988 Check	$14^h57^m46^s.27$	$+00°02'29''.9$	13.236	0.707
1989 Primary	$15^h06^m52^s.15$	$-00°43'26''.5$	12.000	0.818
1989 Check	$15^h05^m51^s.65$	$-00°55'16''.4$	12.578	0.886

Pluto–Charon mutual-event light curves. Our selection of the stars for use before opposition in 1989 is based on observations of 17 stars collected on 1987 April 5 and 6 UT with the 2.24 m University of Hawaii telescope on Mauna Kea. Once again, we chose the two stars having the best combination of brightness, color match, and proximity to Pluto, with the brighter of the two being designated as the primary comparison star. The positions of the two stars were measured on print copies of the Palomar Sky Survey and should be accurate to better than 2 arcsec, although the unknown proper motions could make the 1988 epoch positions somewhat less accurate.

Table III lists the positions and initial magnitude and color measurements for these two stars along with the same information for the 1988 comparison stars, which should be used starting with the May 6 event.

Standardization of the various comparison stars used in previous years is also being continued. Table IV shows the currently adopted magnitudes and colors for the primary comparison stars used in 1988, with the uncertainties shown directly above the magnitudes and colors in units of the least significant digit. These uncertainties represent the standard deviation of the weighted mean of seven nights of observation of 1987 Primary (but only four nights of V magnitude data) and seven nights of data on 1988 Primary. The $B-V$ colors are not exactly equal to the differences between the B and V magnitudes because of the weighting procedure, but the discrepancies are smaller than the uncertainties and can therefore be ignored.

TABLE IV. Standard magnitudes for primary comparison stars used in 1988.

Star	B	V	$B-V$
	12	39	31
1987 Primary	12.3094	11.4265	0.8824
	6	10	11
1988 Primary	12.2571	11.3285	0.9282

V. COMMENTS

This new model for the Pluto–Charon system indicates that the mutual-event season began with the superior event of 1984 December 18 UT; the season will conclude with the inferior event on 1990 October 12 UT, a shift of only one event from the prediction in Paper III. Pluto's first perihelion passage since its discovery will occur on September 5.

Several different experiments can be performed with the geometry produced in 1989. In addition to the expected improvements in the orbital elements for Charon and the radii of both bodies, we have the opportunity to probe the albedo of the south polar region of Pluto and to look for similar latitudinal albedo variegation over the surface of Charon.

1989 may well be the last year during which we will have the opportunity to observe post-eclipse brightening on Pluto. Figure 2 shows the light curve of the 1988 April 18 UT transit of Pluto by Charon and its shadow. The shallow bump around last contact represents our strongest evidence yet for the occurrence of post-eclipse brightening on Pluto. If this phenomenon is due to the deposition of fresh, highly reflective methane frost on some normally lower-albedo surface, such as the equatorial region of Pluto, then the time before opposition is the best time to study this effect. As shown in Fig. 1, by the time of postopposition quadrature, Charon's shadow will have moved away from Pluto's equatorial region, so the best time to secure additional observa-

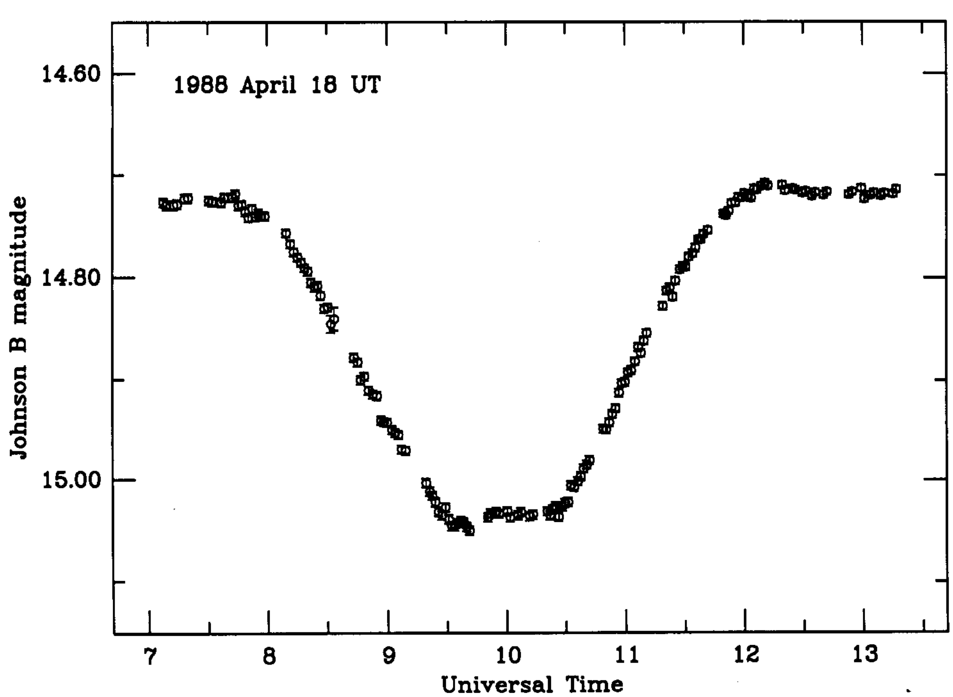

FIG. 2. This light curve of the 1988 April 18 UT transit of Pluto by Charon was obtained by D. J. Tholen with the University of Hawaii 2.24 m telescope on Mauna Kea. The periodic gaps represent times when the comparison star was observed. With two exceptions, the error bars on all points are between 0.0034 and 0.0044 mag. Note the post-eclipse brightening apparent just after 12 hr UT. The size of the effect is less than 0.01 mag, yet the frequency of Pluto and comparison-star observations makes it difficult to ascribe the effect to anything other than an intrinsic brightening of Pluto. The increase in brightness evident at light-curve minimum could be due to the same phenomenon.

tions is around preopposition quadrature. Because of the shallowness of the effect, large-aperture telescopes, dark skies, and superb photometric conditions are required. Such a combination occurs too infrequently for any one observer, so every effort should be made to observe the handful of remaining opportunities.

As noted in Paper III, we strongly urge observers of these events to obtain on the order of an hour of light-curve coverage either before first contact or after last contact, if at all possible. Also, the recommended comparison stars should be observed at least once during each event observation, even if a local (within the field of a CCD) comparison star is utilized as the primary monitor of atmospheric extinction. Careful, high-precision observations of the transformation stars given in Paper III should be made at least once during the opposition to determine the color term for the observer's instrumental system.

Additional comments and some basic guidelines for observing these mutual events can be found in Sec. IV of both Paper I and Paper II, and Sec. V of Paper III.

As before, more detailed circumstances for any particular event can be obtained by writing to the first author. When requesting such information, please specify the nights for which more information is desired and include observatory coordinates so that airmass and twilight information can be properly computed.

We thank W. Nakano for preparing Fig. 1. We also extend our apologies to G. R. Gladstone, whose name was misspelled in the references section of Paper III. The computations that produced the model presented in this paper were performed on the Cray X-MP/48 at the San Diego Supercomputer Center, which is sponsored by the National Science Foundation. This research was supported by NASA grant no. NGL 12-001-057.

REFERENCES

Beletic, J. W., Goody, R. M., and Tholen, D. J. (1988). Icarus (in press).

Binzel, R. P. (1988). Science **241**, 1070.

Birch, P. V., Bowers, C. L., and A'Hearn, M. F. (1988). Aust. Phys. **24**, 222.

Blanco, C., Di Martino, M., and Ferreri, W. (1988). Astron. J. (submitted).

Blow, G. L., and Priestley, J. (1988). IAU Circ. No. 4611.

Buie, M. W., and Tholen, D. J. (1988). Icarus (in press).

Hubbard, W. B., Hunten, D. M., Dieters, S. W., Hill, K. M., and Watson, R. D. (1988). Nature (submitted).

Kilmartin, P. M., Allen, W. H., and Gilmore, A. C. (1988). IAU Circ. No. 4612.

Marcialis, R. L. (1988). Astron. J. **95**, 941.

McKinnon, W. B., and Mueller, S. (1988). Nature **335**, 240.

Mulholland, J. D., and Gustafson, B. Å. S. (1987). Astron. Astrophys. **171**, L5.

Simonelli, D. P., Pollack, J. B., McKay, C. P., Reynolds, R. T., and Summers, A. L. (1988). Icarus (submitted).

Tholen, D. J. (1985a). Astron. J. **90**, 2353.

Tholen, D. J. (1985b). Astron. J. **90**, 2639 (Paper I).

Tholen, D. J., Buie, M. W., Binzel, R. P., and Frueh, M. L. (1987a). Science **237**, 512.

Tholen, D. J., Buie, M. W., and Swift, C. E. (1987b). Astron. J. **93**, 244 (Paper II).

Tholen, D. J., Buie, M. W., and Swift, C. E. (1987c). Astron. J. **94**, 1681 (Paper III).

Tholen, D. J., and Hubbard, W. B. (1988). Astron. Astrophys. (in press).

Watson, R. D., Hill, K. M., and Dieters, S. W. (1988). IAU Circ. No. 4612.